Raman spectroscopic study of bulk water supercooled to − 33 °C

D. E. Hare and C. M. Sorensen
Department of Physics, Kansas State University, Manhattan, Kansas 66506

(Received 7 August 1989; accepted 26 March 1990)

We present Raman spectroscopic measurements in the OH stretch region of water (2900 to 3800 cm^{-1}) for the temperature range 80 to − 33 °C. This latter temperature represents the homogeneous limit of nucleation for our bulk samples. We find that the temperature dependence of both our intensity and depolarization ratio measurements are well described by a two-state model in which both states have frequency dependent depolarization ratios. We argue that the hydrogen bonded mode of the spectrum begins to develop a collective nature at both its low and high frequency ends. This collective nature can explain a breakdown in isosbestic behavior at low temperature. It is suggested that these collective modes may be due to in- and out-of-phase motions of OH oscillators. Their intensity approaches those seen in amorphous solid water as the liquid is cooled to the apparent singular temperature $T_s \simeq -45$ °C, for a variety of bulk properties. We use our Raman data to make an estimate of hydrogen bond probability and show that four bonded molecules would percolate near the singularity. We then argue that the collective mode grows because clusters of four bonded molecules grow in extent until at T_s percolation occurs to yield an infinite cluster with the amorphous solid's collective spectrum.

I. INTRODUCTION

It has been known for quite some time that as water is supercooled below its equilibrium freezing point a large number of thermodynamic and transport properties display anomalous increases, which may be characterized by a power law of the form

$$X \sim (T - T_s)^{-x}, \tag{1}$$

where T_s is the singular temperature roughly equal to − 45 °C for all parameters X.[1–3] That this anomaly is related to the unique hydrogen bonded structure of water is readily apparent through experiments which either destroy or enhance the structure of supercooled water.[4–7] Thus a qualitative picture of open networks of hydrogen bonded water molecules has developed, but the problem still remains as to what specific structures are involved and how they cause the anomaly.

In the past, Raman spectroscopy has proven valuable in the study of water and its hydrogen bonded structure, both in the normal and supercooled regimes. Walrafen has used such data to advocate a two-state model for water.[8–10] This model is supported by his Raman studies of the OH stretch regime which have shown isosbestic behavior indicative of two competing classes of OH oscillators with opposite temperature dependencies. These two classes or states are usually identified as hydrogen bonded (HB) and nonhydrogen bonded (NHB) OH groups.

A number of Raman studies have appeared to study the supercooled regime.[12–19] In general, one finds enhanced hydrogen bonding with declining temperature and some indication that the amorphous solid would be obtained if water would not nucleate for another 100 ° of cooling. D'Arrigo *et al.*[12] have presented data which also show an isosbestic point in support of Walrafen. The isosbestic behavior breaks down, however, in the supercooled regime. Their interpretation is that two states of "open" and "closed" water exist in equilibrium and are analogous to HB and NHB states. In the supercooled regime a third phase, that of heterogeneous ice fluctuations, occurs and upsets the isosbestic behavior. The idea is developed that these ice fluctuations are responsible for the anomaly.[20]

Green, Lacey, and Sceats (GLS) have shown that the low frequency shoulder of the polarized OH stretch spectrum may be developed as a measure of bond–bond correlations in water.[16] They showed after suitable spectral stripping that the relative intensity of this collective mode increased linearly with declining temperature and approached that found in ice or amorphous solid water near the singular temperature T_s. By isotopic substitution with D_2O they also showed that defects in the hydrogen bonded network of liquid water lowered the intensity of the collective mode and then related the defect density to temperature and showed it went to zero near T_s.[17] Thus the physical picture is that as water is cooled the water network of hydrogen bonds becomes more perfect and would reach perfection, i.e., no defects with a structure like that of the amorphous solid at T_s.

Theoretical explanation of the anomaly has taken a number of different tacks. As described above, D'Arrigo has proposed that prenucleation ice clusters form in water and give rise to the anomaly.[20] Speedy has developed a picture wherein T_s represents a limit of mechanical stability as part of a spinodal curve near which critical phenomena behavior is observed.[1,21,22] This description relies less on direct structural information and more on thermodynamic arguments. Stanley and co-workers[23–25] have developed a site percolation model in which the hydrogen bonded network is viewed as gel-like over suitably short time scales. As the probability of hydrogen bonding increases, patches of four bonded water molecules occur with greater frequency until these four bonded molecules percolate, i.e., form an infinite cluster at T_s. The anomaly is then associated with the concomitant entropy and density fluctuations that grow with these clusters. In a more general vein, numerous speculations have

 0021-9606/90/130025-09$03.00

occurred regarding the structure of water patches, whether they are ice-like or clathrate-like,[4,5,26] the importance of ring structures,[27] and fivefold symmetry.[28] Experiments are hard pressed to differentiate between these reasonable propositions.

In this paper we present Raman studies of the OH stretch spectrum of water. Experimentally, our work may be differentiated from earlier work in two ways. First, by using a special method of capillary filling, we have obtained spectra for water to -33 °C in bulk samples. This is significantly colder than any previous work. Second, we pay attention to making accurate depolarization measurements as a function of frequency and temperature. Our analyses include the GLS stripping procedure to find the collective mode and a consistency analysis for the isosbestic point. We find that the temperature dependence of our intensity and depolarization data can be adequately explained using a two-state model. We also find that the water spectrum appears to be approaching that of the amorphous solid as the system is cooled. We combine all these results and use percolation concepts to indicate that collective modes, both at low and high frequencies, do begin to become strong as water is supercooled because as the probability for hydrogen bonding approaches the four bonded percolation threshold, large clusters with the structure of amorphous water form with size diverging at T_s.

II. EXPERIMENTAL METHOD

A. Preparation and properties of the samples

The samples consisted of pure liquid water contained in Mossop Capillaries.[29] Two desirable characteristics resulted from this method of preparation:

(1) The samples can be shown to be essentially free of surface effects due to their small surface to volume ratio.[30]

(2) Their great purity allowed supercooling to their homogeneous nucleation limit (approximately -34 °C for these samples).[29]

Our method of sample preparation[30] was similar to that used by Mossop.[29] The apparatus was a distiller constructed to purge a 3 mm i.d. (5 mm o.d.) hard Pyrex tube with saturated steam for about 2.5 h. The tube was then pulled to a capillary in an oxy-methane torch while steam continued to pass through the tube. After pulling, the end was flame sealed, water condensed into the capillary, and when sufficient water had condensed, the tube was removed and sealed at its other end with the torch. At no time after the purge commenced did the interior of the tube become exposed to anything but liquid water and its vapor. The result is high purity water contained by a fresh Pyrex surface that has never been exposed to the atmosphere.

The typical capillary which resulted was roughly 300 μm in i.d. (500 μm in o.d.) and was about 5 cm in length. About 1 cm of vapor space was left at one end to allow for thermal expansion of the sample. If the sample was correctly sealed, the only contents were water and its vapor, and the only pressure on the sample at any time was the vapor pressure of water.

After a batch of samples was made, the sample ends were examined under low power magnification and a sample was rejected if a microleak was seen. The survivors were loaded into a refrigerated methanol bath and taken down to about -32 °C for several minutes. Usually about 10% to 20% of the original batch did not nucleate and it was from this tiny subset that a Raman sample was finally chosen. Good optical qualities such as a high degree of cylindrical symmetry, relatively large i.d., and a uniform and not too thick glass wall were important in making the final selection.

Density measurements have previously demonstrated that 300 μ i.d. capillaries show negligible surface effects, yet such capillaries are small enough to homogeneously nucleate around -34 °C.[30] Because this technique will routinely prepare samples of these dimensions that are free of heterogeneous nuclei, it is very useful for extending our knowledge of some of the bulk properties of liquid water down to these low temperatures.

B. General description of the Raman setup

Excitation was accomplished with an Ar^+ laser operating at 4880 Å with about 70 mW of plane polarized output. This output was focused down to a narrow waist beam with a 12.4 cm focal length lens and the sample was located at the focal point with its axis of cylindrical symmetry parallel to the electric field polarization of the incident beam (vertical).

The scattered light was collected and collimated by an $f/1.7$ lens with its axis passing through the scattering volume and perpendicular to both the incident beam and its electric polarization. The image was condensed and passed first through a polarized analyzer (extinction ratio $<10^{-3}$) and then a calcite double wedge polarization scrambler before passing into the spectrometer. The analyzer could be accurately rotated to allow for detection of either vertically, I_{VV}, or horizontally, I_{VH}, scattered light.

The spectrometer was a Spex 1404, 0.85 m double monochromator. Detection was accomplished with a Hamamatsu R943-02 photomultipler tube (PMT) which was refrigerated to -30 °C to suppress thermal electron noise. The spectrometer was operated with a bandpass of 15 cm^{-1} and the width of a channel in the digitized spectra was also 15 cm^{-1}. The PMT output was discriminated and shaped by a PAD. The resulting shaped pulse output was counted and stored by a computer where it could be easily manipulated and plotted.

The capillary sample was contained in a specially constructed copper cell. An outer sleeve was maintained at approximately the sample temperature to suppress strong thermal gradients near the sample. Thermal contact of the scattering volume was obtained principally by dry nitrogen which oozed out directly over the sample after coming to the cell temperature. Temperature was monitored by a thermistor housed in a hole drilled into a solid copper rod which was soldered right next to the nitrogen outlet. The entire cell was housed in a small pine box insulated with styrofoam. The laser beam entered and exited through two small plane glass side windows and the collection lens was mounted directly into the front of the box. Temperature control of the cell was

accomplished by methanol or water pumped from a temperature control bath.

C. Digital spectral corrections

The following and only the following corrections were performed on the raw data.

Counter saturation could occasionally be a problem as the count rate would deviate significantly from direct proportionality with the input intensity at large count rates. We corrected this problem with a program which used an empirically determined calibration to map the observed count rate into the true count rate. In addition, we never allowed the count rate to go into a region in which the observed value differed from the true value by more than 3% thus ensuring that the correction was relatively small.

Our entire apparatus from the collection lens back to the PMT was calibrated against an NBS traceable standard lamp.

It was necessary to separate the scattering due to water from the background, which was almost entirely due to either the Raman scattering or fluorescence of the Pyrex capillary. It was assumed in the removal procedure that the intensities at 2635 and 4098 cm^{-1} were, at all temperatures, due entirely to Pyrex and other types of noise. This is only approximately correct as detectable combination intensity in water exists at both frequency limits.[31] However, in comparison to the OH stretch feature these other bands have negligible intensity and the assumption is useful. The uncertainty in this correction forms the principal uncertainty in the spectra, especially the fairly low intensity VH spectra.

Figure 1 shows our results for both polarizations and most of the measured isotherms between -33.0 and 80 °C. Unfortunately, we found large random errors in our -33.0 °C isotherm for I_{VH} and hence do not include those data here.

One additional correction was used when we calculated the hydrogen bond probability (below). This was the Placzek correction[32]

$$I_{pc}(\nu) = I_{obs}(\nu)K(\nu) \tag{2}$$

with

$$K(\nu) = \nu[1 - \exp(-h\nu/kT)](\nu_L - \nu)^{-4}. \tag{3}$$

Here ν_L is the incident laser frequency, I_{obs} is the observed spectrum, and I_{pc} is the Placzek corrected spectrum. Certain frequency biases inherent in the Raman scattering process are accounted for by this correction. Thus the I_{pc} spectrum more clearly represents relative populations of the HB and NHB scatterers than I_{obs} does. This correction was not used for any of the other results or figures.

D. Accuracy of the results

The intensity uncertainty was principally due to background removal. This has been estimated to be about $\pm 5\%$ of peak intensity for a VH spectrum and $\pm 1\%$ of peak intensity for a VV spectrum.

Each reported spectrum is the average of at least ten scans. For each isotherm, the individual VV and VH scans were taken in an alternating sequence to ensure that a definite intensity relationship existed between the final VV and VH spectra of the same isotherm. Careful alignment failed to completely remove a slight frequency independent bias in favor of the VH spectra. This bias was determined by measuring the depolarization ratios of known depolarized Raman lines of CCl_4, C_6H_6, and C_6H_{12} (cyclohexane), and an unpolarized source. These samples were all contained in capillaries of the same size as the water containing subjects of this experiment. It was found that multiplication of the VV spectra by 1.074 ± 0.02 yielded correct depolarization ratios for these lines.

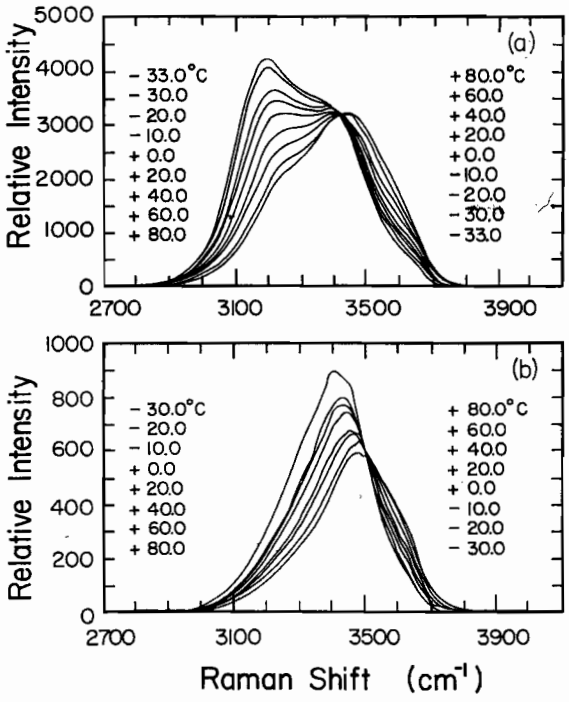

FIG. 1. (a) VV spectra; (b) VH spectra. For display purposes, the VV were all normalized to cross at 3403 cm^{-1}, the Walrafen isosbestic. The VH spectral isotherms take the same normalizations given to the VV and relative intensity between any VV, VH isotherm pair is correct. The -33.0 °C VH spectrum was left out because of its poor quality.

Our small scattering volumes and low laser intensity necessitated the use of a large $f/1.7$ collection angle. Previous authors have worried about the dangers involved in using large collection angles as this tends to alter depolarization information.[33] This scrambling is most evident when measuring very highly polarized Raman lines. Both calculation of this effect and measurements of the depolarization of the highly polarized line of CCl_4 at 459 cm^{-1} indicated that the effect of the $f/1.7$ collection aperture is an order of magnitude smaller than uncertainties from the VH background. Furthermore, our depolarization calibration described above corrects for this effect. Our reported depolarization ratios are accurate to about $\pm 5\%$ in the region 3400 to 3500 cm^{-1} although accuracy falls off towards the 3100 or 3650 cm^{-1} limits.

We were also concerned with temperature accuracy. Laser heating of the sample was demonstrated to be negligible by measuring the melting point of a frozen water sample by Raman spectroscopy of the OH stretch using the same incident power, etc., as in the data acquisition. The thermistor was calibrated against NBS traceable Hg in glass thermometers before a set of runs, as well as verifying calibration via the same method afterwards. Correct calibration of the thermistor and absence of a temperature gradient between the thermistor position and the scattering volume was verified at the highest and lowest temperatures by visual melting point measurements on naphthalene and CCl_4 samples of previously and independently measured melting point. The temperature at all reported ranges is accurate to ± 0.5 °C.

III. ANALYSIS

A. The GLS analysis

Green, Lacey, and Sceats[16] (GLS) proposed an insightful analysis in which the liquid water OH stretch spectra were viewed as being more ice-like, and less like perturbations on highly localized vapor-like modes. In particular, the highly polarized, low frequency shoulder occurring in the VV spectra at roughly 3200 cm^{-1} was identified as being essentially of the same origin as the intense ν_1 in phase Raman band found in ice at 3083 cm^{-1}.[34] This mode maybe visualized as the in-phase symmetric stretching of H_2O molecules in the lattice. In the GLS work, the relative intensity of this "collective" mode was developed as an indicator of the extent to which strong and uniform hydrogen bonding exists in the liquid. These authors reasoned that an adequate method of removing this collective mode from the total VV intensity was to strip it away with the VH spectrum of the same isotherm, the principal assertion being that the VH spectrum was a scaled down version of what the VV would look like without the collective contribution. The ratio of this integrated collective intensity to the integrated intensity of the VV isotherm from which it came was defined to be $C(T)$. This function was further refined by assuming symmetry of the collective peak about its maximum. The high frequency side of the final symmetrized collective intensity was derived by reflection of the low frequency side about the maximum.

We have attempted to reproduce and extend to lower liquid temperatures the GLS results. The collective mode I_c was calculated with

$$I_c(\nu,T,\delta) = I_{VV}(\nu,T) - aI_{VH}(\nu+\delta,T). \quad (4)$$

The VH spectra may be manipulated both by scaling with a and by frequency shift δ before subtraction from I_{VV}.[35] The δ was chosen which best symmetrized I_c prior to its reflection symmetrization. Finally this preferred I_c was reflection symmetrized and $C(T)$ formed from it. The values of C(T) we obtained are shown in Fig. 2 (closed triangles) where they are compared to the GLS results with good agreement.

One problem with this analysis, we believe, is the use of the frequency shift parameter δ which increases uniformly from 0 cm^{-1} at -30 °C to 35 cm^{-1} at 80 °C. This parameter is without physical basis although its use is necessary for the nice linear behavior of $C(T)$. We have performed the GLS analysis with $\delta = 0$ at all T using both no symmetrization and symmetrization and plot these results in Fig. 2 as well. In either case the linear behavior is lost and the agreement with GLS at large temperatures is poor. Visual inspection of the stripping procedure has shown us that δ is necessary at large T to match the peak of the VH spectrum and the high frequency VV spectrum. Without this match, $C(T)$ includes parts of the high frequency spectrum which is inconsistent with the original concept of GLS. Thus it may be that δ is indeed unphysical and merely an esthetic convenience to ensure "proper" stripping. This does not imply that the concept that the low frequency edge is some sort of collective mode is wrong, but rather there is nothing special about the GLS stripping procedure. To illustrate this, we have applied a simple analysis of graphically removing the low frequency "bump" from the spectrum by eye with pen and ruler and measuring its area. This method, with results also shown in Fig. 2, while unsophisticated is intuitive and simple and yields a clean indication of a collective mode with increasing intensity approaching that of ice or amorphous solid water near the singularity temperature in liquid water. Hence we feel the ideas expounded by GLS, that this collective mode grows with declining T and approaches that found in ice Ih or the amorphous solid and is an indicator of the structure responsible for the singularity, are correct.

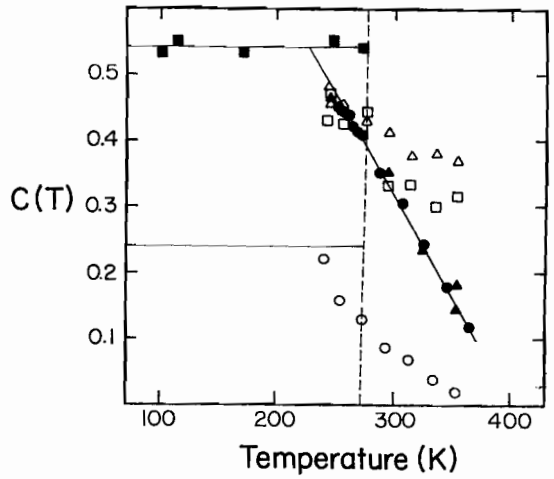

FIG. 2. The $C(T)$ function representing relative intensity of the collective mode. The points ■ and ● are derived from ice and liquid water, respectively, and are taken from the GLS work. The remaining symbols represent various methods of calculating $C(T)$ from the data of our work. The △ were produced from nonsymmetrized collective spectra. Frequency shifting of the VH relative to its VV isotherm was not allowed. The □ are symmetrized with no shift allowed. The ▲ were symmetrized and frequency shifting was allowed if this improved the fit. This is the method used by GLS. For the ○ points, collective intensity was separated from the VV spectra by a pen and ruler. The horizontal line at $C(T) = 0.24$ is the value obtained from the amorphous solid by this procedure.

B. Depolarization ratios

Our depolarization ratio results are displayed in Fig. 3. The principal limit on ratio accuracy was the low VH intensity relative to the VH uncertainty due to Pyrex fluorescence/Raman removal. For this reason the ratio is not re-

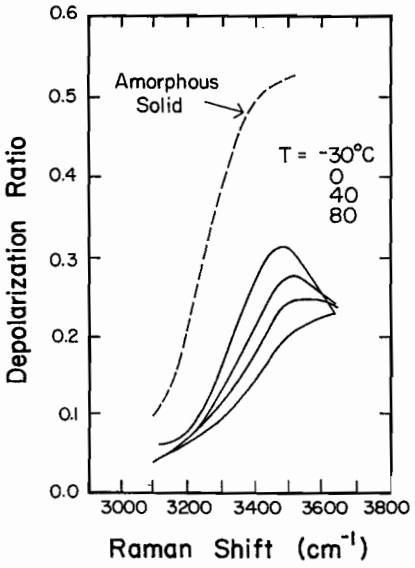

FIG. 3. The temperature and frequency dependence of the depolarization ratio of liquid water. Also shown for comparison is the depolarization ratio of amorphous solid water at 100 K.

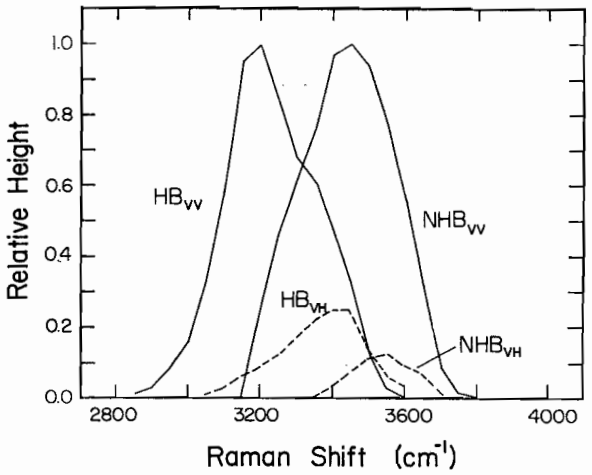

FIG. 4. The fundamental hydrogen bonded and nonhydrogen bonded shapes derived from a two-state assumption.

ported below 3100 cm^{-1} or above 3650 cm^{-1} as the results rapidly become spurious beyond these limits. Fortunately, the region of least uncertainty (3400 to 3500 cm^{-1}) agrees well with earlier measurements[10] at a single temperature and also shows a rather remarkable trend indicating an increase in depolarization ratio with decrease in temperature. As will be shown, this result can be explained by a two-state model, but one must have a frequency dependent depolarization ratio in each band. Also drawn in Fig. 3 is the depolarization ratio of the amorphous solid.[36] This curve may be only qualitatively correct because the data are difficult to obtain.[37] Our data show a distinct and suggestive trend toward this amorphous solid result.

C. Intensity ratios in a two-state model

Consider a very simple two-state model. Raman scatterers are classified in two categories labeled hydrogen bonded scatterers (HB) and nonhydrogen bonded scatterers (NHB). Generally, the HB scatterers make up the lower frequency shift intensity, and conversely the NHB dominate the higher frequency. There is considerable overlap, however, so that scattering at the median frequencies is due to both:

$$I(\nu,T) \propto \sigma_{\mathrm{HB}}(\nu)\Omega_{\mathrm{HB}}(\nu)\exp(-E_{\mathrm{HB}}/kT) + \sigma_{\mathrm{NHB}}(\nu)\Omega_{\mathrm{NHB}}(\nu)\exp(-E_{\mathrm{NHB}}/kT). \quad (5)$$

In Eq. (5) Ω is the density of states, σ is the Raman cross section, and k is Boltzmann's constant. An equality may be formed if we divide by the intensity at a ν_0 chosen low enough to ensure its intensity to be entirely due to the HB scatterers. Then the ratio has the form

$$\frac{I(\nu,T)}{I(\nu_0,T)} = a(\nu,\nu_0) + b(\nu,\nu_0)\exp(-\Delta E/kT), \quad (6)$$

where $\Delta E = E_{\mathrm{NHB}} - E_{\mathrm{HB}}$.

The labeling of the two categories is deliberately ambiguous. We do not wish to speculate in this section on the structure of the scattering units we call HB and NHB scatterers, nor is it necessary to do so in the following analysis. It is necessary to assume that the HB scatterers are all in a lower energy state than the NHB scatterers and that this energy difference is well defined. It is convenient to assume that the scatterers act independently and therefore scatter incoherently thus preserving a simple relationship between the number of scatterers and the scattering intensity. For the HB scatterers at low T this is clearly an assumption of convenience and is in fact inconsistent with the concept of a collective mode. Thus when examining the results of this analysis we shall be aware of the weakness of this assumption and its possible consequences.

The slope of log $[I(\nu,T)/I(\nu_0,T)]$ vs. $1/T$ plots can yield good estimates of the two Raman modes of the two-state model, $I_{\mathrm{HB}}(\nu)$ and $I_{\mathrm{NHB}}(\nu)$. The slope is given by the derivative of the logarithm of Eq. (6) with respect to T^{-1} which is

$$\text{slope} = -\frac{\Delta E}{k}\frac{I_{\mathrm{NHB}}(\nu,T)}{I_{\mathrm{HB}}(\nu,T) + I_{\mathrm{NHB}}(\nu,T)}. \quad (7)$$

The curvature of these plots over our $1/T$ domain was very gentle. Given this, we let the slope from the data represent the value of this derivative at the median value of $1/T$. This combined with $I_{\mathrm{Total}} = I_{\mathrm{HB}} + I_{\mathrm{NHB}}$ allowed us to extract the individual Raman intensities.

This extraction was done using a value of $\Delta E = -2.8$ kcal/mol, a reasonable mean of various estimates in the literature,[8,10,13] at three different temperatures, -30, 10, and 80 °C, and the line shapes agreed very well. The average normalized line shapes for both polarizations are shown in Fig. 4. For both HB and NHB modes the peak of the VH is at higher frequencies than the VV. Also, the depolarization ratio of the HB mode approaches unity in this regime which is greater than the theoretically allowed 0.75. We do not consider this a serious problem, however, given the estimates

involved in the extraction procedure. These shapes compare well to those obtained by D'Arrigo *et al.*[12] using a different procedure.

D. A self-consistency test of the isobestic hypothesis

Walrafen, Hokmabadi, and Yang[9] have performed careful measurements to show that the OH stretch Raman spectra of liquid water exhibit isosbestic points. D'Arrigo *et al.*[12] have also found an isosbestic point in the OH stretch spectra, but indicated that the isosbestic behavior failed in the supercooled region. They attributed this breakdown to the appearance of a third group of scatterers near 3150 cm^{-1} in the supercooled liquid.

Accurate relative intensity measurements between different isotherms are very difficult to achieve with capillaries, and we made no attempt to do so. Hence isosbestic points could not be determined directly. However, it was a fairly simple matter for us to obtain the correct intensity relationship between the VH and VV spectra of the same isotherm. This allowed us to use a self-consistancy scheme to explore the isosbestic behavior. Walrafen *et al.* observed that the VV spectra cross at their isosbestic frequency of 3403 cm^{-1}. We forced our VV spectra to cross at 3403 cm^{-1} by multiplying each spectral isotherm by a constant $a(T)$. Because a consistent relationship does exist between our VV and VH results, the scaling of each $I_{VH}(\nu,T)$ by the same isotherm unique $a(T)$ will likewise force the relative normalization of all VH spectra. Then we must have all these $a(T)$ scaled VH spectra crossing at the VH isosbestic frequency of 3523 cm^{-1} reported by Walrafen *et al* to retain a consistent picture.

The data in Fig. 1 were normalized in this manner and one can barely see a breakdown in the isosbestic behavior in the VH spectra for low temperature. To show this better we plot in Fig. 5 the relative difference of the scaled $I_{VH}(T)$ and $I_{VH}(+20.0\,°C)$ at 3523 cm^{-1} against T. Except for the point at 70.0 °C, the points from 0.0 to 80.0 °C scatter very satisfactorily within $\pm 3\%$ of zero. Points below 0.0 °C show increasing positive deviation and the -20.0 and -30.0 °C points deviate by 10% which is outside our experimental error based on background removal errors. It is reasonable to attribute this to the failure of the isosbestic behavior to be maintained in the supercooled region as D'Arrigo *et al.* have concluded.

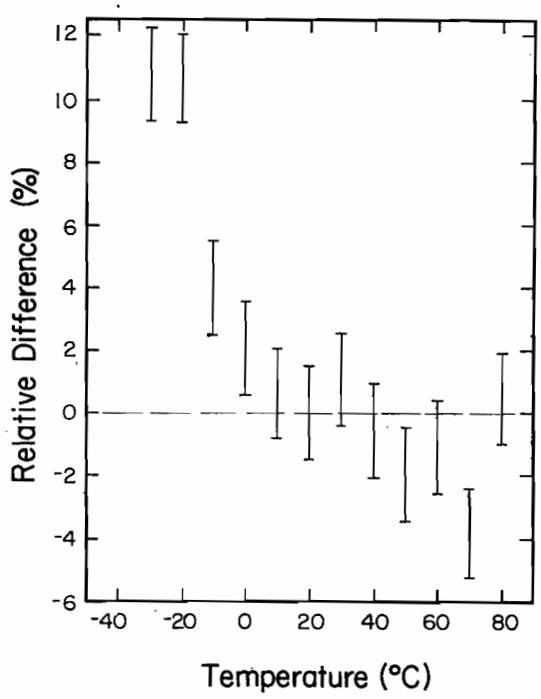

FIG. 5. Relative intensity difference between the 20 °C VH isotherm and the other rescaled VH isotherms at 3523 cm^{-1} $[I_{VH}(20\,°C) - I_{VH}(T)]/I_{VH}(20\,°C)$.

IV. DISCUSSION

In this section we will use our experimental results to support a two-state interpretation of our data in which the lower frequency, hydrogen bonding state is approaching that of collective modes similar to those in amorphous solid water. We use this two-state model to make an estimate of the hydrogen bond probability and show that this probability crosses the four bonded percolation threshold in the region of the singular temperature T_s. We then argue that at this threshold infinite clusters of four bonded molecules appear and hence can explain the apparent onset of amorphous water collective mode behavior at the singularity.

The depolarization ratio results shown in Fig. 3 will support a two-state model of liquid water although the simplest model of this sort fails. Such a model would assume two pure states, HB and NHB, each with its own frequency independent depolarization ratio ρ. From Fig. 3 we see the low frequency ρ is less than the high frequency limit of ρ; these limiting frequency regimes correspond to essentially pure HB and NHB states, respectively. Thus we would assign $\rho_{HB} < \rho_{NHB}$. Given this we expect that at some intermediate frequency where both HB and NHB modes contribute ρ would fall with declining temperature which enhances HB over NHB states. This is not observed in Fig. 3 so this simple model does not work.

A two-state model can be made to work if we relax the assumption of constant ρ across either band. If ρ for both HB and NHB states was largest at the high frequency edges of both bands, then the behavior in Fig. 3 can be qualitatively explained. The spectral deconvolution procedure described in Sec. III led to HB and NHB modes shown in Fig. 4. The depolarization ratio is indeed largest at the high frequency ends of each mode as required to explain the total depolarization ratio discussed above. Thus the intensity ratio analysis and the depolarization ratio analysis are mutually consistent with a two-state interpretation.

We now ask, what is the nature of this hydrogen bonded mode? In Fig. 6 we plot a comparison of the deconvoluted HB mode with the spectrum of amorphous solid water[36,38]; the shapes are similar. Both exhibit a VV peak in the range 3150–3200 cm^{-1} with a large shoulder at higher frequency. Walrafen[10] assigned a mode at 3210 cm^{-1}, which matches

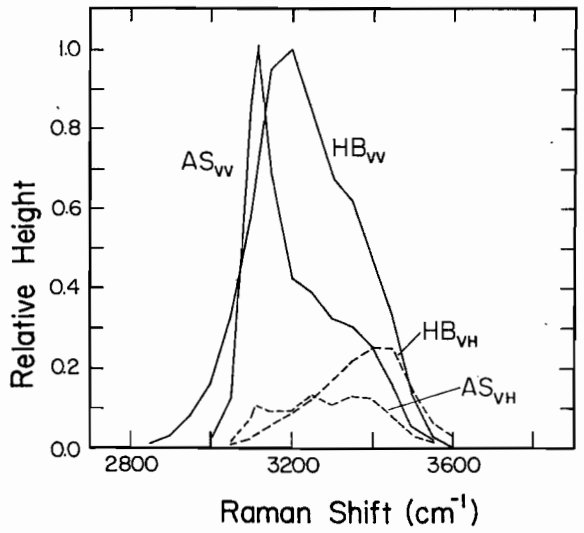

FIG. 6. Comparison of the hydrogen bonded VV and VH shapes extracted under the two-state assumption from our liquid water data (HB_{VV} and HB_{VH}) to the VV and VH Raman spectra of the amorphous solid at 100 K (AS_{VV} and AS_{VH}). The slight peak in AS_{VH} at about 3120 cm^{-1} is probably spurious, the result of leakage from the intense VV spectrum.

well with our HB_{VV} peak, to collective in-phase stretching motions of aggregates of H_2O molecules. The mode near 3150 cm^{-1} in ice Ih and amorphous solid water is the ν_1 (symmetric stretch) in phase collective mode. Thus we conclude the hydrogen bonded mode in supercooled water, seen in Fig. 6, is a collective in-phase mode similar in character to that seen in the solid phase. It is the growth of this mode with decreasing temperature in liquid water which was implicated by GLS as approaching the same intensity as that of ice Ih or the amorphous solid near the singular temperature. Our results using the GLS analysis (Fig. 2) are consistent with this interpretation.

Figure 6 also demonstrates a reasonable match in the VH spectra between the amorphous solid and the HB mode. This is emphasized in Fig. 3 where the depolarization ratio as a function of frequency for the amorphous solid is compared to our results for water at various isotherms. It is reasonable to infer that liquid water's depolarization ratio is approaching that of the amorphous solid as the temperature is lowered. Whalley[34] has assigned ν_1 out of phase to the region 3400–3500 cm^{-1} in amorphous solid water. This is where our depolarization ratio peaks at low temperature. Given this and the collective ν_1 in phase assignment near 3150 cm^{-1}, it is very reasonable to suggest that we are observing another distinctly different strongly coupled mode (perhaps ν_1 out of phase) in liquid water as well. Hence, especially at low temperature, the nature of the HB mode of liquid water is that it displays two or more modes of a collective nature similar to those found in the amorphous solid.

The main experimental proponent of the two-state model is the isosbestic behavior observed in the OH stretch region. Walrafen[8] has over the years strongly advocated this model and recent careful measurements[9] strongly support the existence of an isosbestic. One of the conditions necessary for isosbestic behavior in the two-state model is that the scattering intensity should be directly proportional to the scattering population, at least at the isosbestic frequency. If the fundamental scattering units are single H_2O molecules, this will hold true as long as the scatterers are vibrating incoherently with respect to each other. This is clearly incompatible with what is meant by a collective mode. Note that a collective mode has the potential either to enhance or suppress the intensity depending on whether constructive or destructive scattering interference is taking place at the intermolecular level. For ν_1 in phase, the effect would clearly be enhancement. This would very nicely explain the anomalous intensity growth found at 3150 cm^{-1} by D'Arrigo *et al.* as temperature is decreased into the supercooled region. Examination of their Fig. 2 also shows that the -24.0 °C isotherm of $I_{VV} - 4/3I_{VH}$ clearly undershoots the isosbestic crossing at 3370 cm^{-1} exhibited by the higher temperature isotherms. This would indicate suppression of HB scattering intensity in the supercooled region at 3370 cm^{-1} which is near the new, possibly ν_1 out-of-phase, mode mentioned above. It is reasonable to expect that as this mode's collective character grew its relative intensity would not increase as fast as the population. It seems that we are witnessing a transition from incoherent scattering of the HB molecules to scattering characterized by significant collective character as we pass into the supercooled region.

Given the concept of a two-state model, we can proceed to calculate the probability that a given OH oscillator is in the hydrogen bonded state P_{HB} by comparing the intensities of the hydrogen bonded mode to the total Raman mode. Such a procedure has, of course, a long history, and often wide variation of P_{HB} is found from various sources in the literature. This variation is the result of the assumptions necessary to determine P_{HB}. In our case these assumptions involve how the Raman cross sections for the HB and NHB states compare, a value for the hydrogen bond energy of 2.8 kcal/mol, and speculation on the structure of the units HB and NHB. The second assumption is a reasonable value from the literature[8,10,13] but may vary by $\sim \pm 0.5$ kcal/mol and hence cause some variation in our P_{HB}. With regard to the first assumption, the data of D'Arrigo *et al.* show that the total Raman intensity due to both modes is independent of temperature for $T > 0$ °C and increases only slightly (15%) by -24 °C. This implies the Raman cross sections are equal. On the other hand, both Walrafen *et al.* and Bansil *et al.* have indicated that the HB oscillators scatter 1.7 greater than the NHB. We have used both these possibilities in computing P_{HB} shown in Fig. 7 and also include other estimates from the literature derived from both Raman[8] and thermodynamic arguments.[39] Considering the last assumption, the simplest model would be to consider the fundamental units as the OH oscillators themselves. Then each HB oscillator counts for one intact bond and each NHB for one broken bond. This implicitly assumes that intramolecular coupling can be ignored. This coupling of two similar oscillators is sufficient to produce such coherent cancellation effects as the apparent absence of the antisymmetric stretch in the Raman spectrum of the vapor. Thus this structural assumption, while simple is not entirely satisfactory.

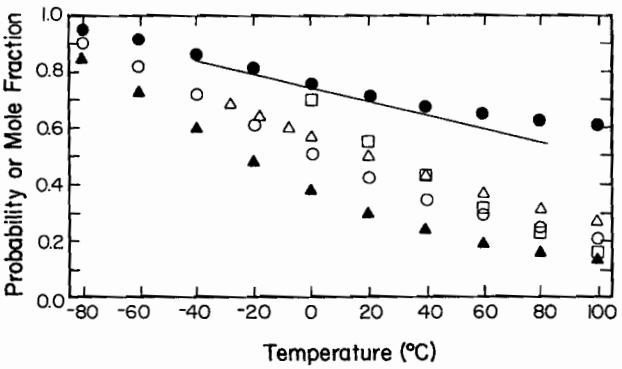

FIG. 7. Hydrogen bond probability P_{HB} calculated in a variety of ways: ○ assume HB and NHB cross sections are equal; ▲ assume HB has 1.7 times larger cross section than NHB; ● assume HB and NHB cross sections are equal and according to Scherer *et al.* (Ref. 40) HB implies two hydrogen bonds per molecule, NHB implies one; △ Raman result from Ref. 12; □ Raman result from Ref. 8; solid line, thermodynamic estimate from Bertolini *et al.* (Ref. 39).

The next step in complexity is to consider the fundamental scattering unit to be a water molecule. This allows for intramolecular coupling, but makes bond counting more ambiguous. The simplest approach of this type is the model used by Scherer *et al.*[40] in which the HB scatterer is a molecule in which both OH oscillators are hydrogen bonded and the NHB scatterer has one of its oscillators bound, the other free. Species having both oscillators unbound are considered insignificant at the temperatures studied. Then each NHB unit counts for one intact and one broken hydrogen bond while each HB unit counts for two intact bonds. We used both approaches in Fig. 7. Certainly there is considerable amibiguity and we can at best only expect a semiquantitative result. The result in Fig. 7 is interesting, however, in that on the average all these different predictions suggests that $P_{HB} = 0.8$ in the temperature regime of the singular temperature T_s. This value for P_{HB} is that required for percolation of the four bonded water molecules. This lends support to the percolation theory that proposes the water anomaly is due to a percolation transition of four bonded water molecules at T_s.[23–25]

This viewpoint can be enhanced by considering the proposed collective modes in the Raman spectrum. As discussed above, both the GLS analysis and our depolarization ratio measurements have led us to conclude that the HB mode is approaching the spectrum of amorphous solid water as the temperature is lowered. If we now combine this with the four bonded percolation occurring in the same regime, we can propose that as $T \to T_s$ and $P_{HB} \to 0.8$, larger and larger clusters of the amorphous solid grow causing $C(T)$ to grow. At percolation, an infinite cluster occurs and $C(T)$ equals that found in an infinite network of amorphous ice.

GLS have argued against the percolation model interpretation.[17] Their measurement of the defect density in the water network goes to zero at T_s. If this defect density is for all the water molecules available, then their conclusion is correct since percolation would occur at a defect density of about $0.2 = 1 - P_{perc}$ which occurs far above T_s. On the other hand, we would propose that this defect density is not for all the molecules but only those in the incipient infinite cluster about to form at T_s. When the defect density is zero, an infinite cluster forms, but P_{HB} for all the water molecules is still only 0.8. This interpretation is supported by Fig. 7 which can be read to show that NHB Raman scattering would still be present at T_s to indicate the existence of defects in the GLS sense. Our interpretation requires that an infinite percolation cluster have the same $C(T)$ as the amorphous solid.

V. CONCLUSIONS

We have presented Raman spectroscopy data in the OH stretch region on bulk samples of water in the temperature range -33.0 to $+80$ °C. This former temperature represents the homogeneous nucleation limit for our samples. We have shown that the temperature dependence of both our depolarization ratio and intensity results are well described by a relatively simple two-state model in which both states have a frequency dependent (but temperature independent) depolarization ratio. In this context we then present arguments that the hydrogen bonded state spectrum is approaching that of amorphous solid water as the temperature is lowered to the singular temperature T_s of the various anomalies that have been observed in supercooled water. We do this in two ways. First we reproduce the analysis of Green, Lacey, and Sceats that a collective mode near 3150 cm^{-1} has a relative intensity that approaches that found in ice Ih or the amorphous solid near T_s. This mode can be assigned to the ν_1 in phase motion in the amorphous solid. Second, we show that our depolarization ratio measurements approach those of amorphous solid water as temperature falls and suggest this is due to another distinctly different, strongly coupled mode near 3500 cm^{-1}, perhaps ν_1 out of phase. We also present consistency arguments that the isosbestic behavior breaks down in the supercooled regime supporting the result of D'Arrigo *et al.* We propose, however, that this breakdown is not due to ice fluctuations as proposed by D'Arrigo *et al.*, but rather is due to the collective nature which causes the Raman intensity to deviate from direct proportionality to the HB population. Finally, we use the two-state model and our Raman data to lend strong support to the percolation theory of the singularity in supercooled water. We use our data and the two-state model to determine the hydrogen bond probability P_{HB}. We show semiquantitatively that P_{HB} approaches the four bonded percolation threshold in the region of the singular temperature T_s. We then support this percolation concept by recognizing that clusters of four bonded molecules would grow and become infinite at the percolation threshold. These clusters would display collective modes, similar to the amorphous solid if they have that structure, and these modes would grow and become equal to that of the amorphous solid when the clusters become infinite at percolation, at T_s.

ACKNOWLEDGMENTS

We thank M. G. Sceats and J. P. Devlin for correspondence regarding their work. We would like to thank Basil

Curnutte for helpful discussions on water structure and its vibrational spectroscopy. Acknowledgement is made to the donors of The Petroleum Research Fund, administered by the American Chemical Society, for partial support of this research and NSF Grant No. CHE 8618576.

[1]R. J. Speedy and C. A. Angell, J. Chem. Phys. **65**, 851 (1976).
[2]C. A. Angell, in *Water: A Comprehensive Treatise*, edited by F. Franks (Plenum, New York, 1982), Vol. 7.
[3]C. A. Angell, Annu. Rev. Phys. Chem. **34**, 593 (1983).
[4]B. L. Halfpap and C. M. Sorensen, J. Chem. Phys. **77** 466 (1982).
[5]C. M. Sorensen, J. Chem. Phys. **79**, 1455 (1983).
[6]R. J. Speedy, J. A. Ballance, and B. D. Cornish, J. Phys. Chem. **87**, 325 (1983).
[7]M. Oguni and C. A. Angell, J. Phys. Chem. **87**, 1848 (1983).
[8]G. E. Walrafen, in *Water: A Comprehensive Treatise*, edited by F. Franks (Plenum, New York, 1972), Vol. 1, Chap. 5, and references therein.
[9]G. E. Walrafen, M. S. Hokmabadi, and W.-H. Yang, J. Chem. Phys. **85**, 6964, 6970 (1986).
[10]G. E. Walrafen, in *Structure of Water and Aqueous Solutions*, edited by W.A.P. Luck (Verlag Chemie, Weinheim, 1974).
[11]For a review see H. S. Frank, in *Water: A Comprehensive Treatise*, edited by F. Franks (Plenum, New York, 1972), Vol. 1; D. Eisenberg and W. Kauzmann *The Structure and Properties of Water* (Oxford, London, 1969).
[12]G. D'Arrigo, G. Maisano, F. Mallamace, P. Migliardo, and F. Wanderlingh, J. Chem. Phys. **75**, 4264 (1981).
[13]R. Bansil, J. Wiafe-Akenten, and J. L. Taaffe, J. Chem. Phys. **76**, 2221 (1982).
[14]S. Krishnamurthy, R. Bansil, and J. Wiafe-Akenten, J. Chem. Phys. **79** 5863 (1983).
[15]Y. Yeh, J. H. Bilgram, and W. Kanzig, J. Chem. Phys. **77**, 2317 (1982).
[16]J. L. Green, A. R. Lacey, and M. G. Sceats, J. Phys. Chem. **90**, 3958 (1986).
[17]J. L. Green, A. R. Lacey, and M. G. Sceats, Chem. Phys. Lett. **130**, 67 (1986).
[18]J. L. Green, A. R. Lacey, and M. G. Sceats, J. Chem. Phys. **86**, 1841 (1987).
[19]J. L. Green, A. R. Lacey, and M. G. Sceats, Chem. Phys. Lett. **137**, 537 (1987).
[20]G. D'Arrigo, Nuovo Cimento B **61**, 123 (1981).
[21]R. J. Speedy, J. Phys. Chem. **86**, 982 (1982).
[22]R. J. Speedy, J. Phys. Chem. **91** 3354 (1987).
[23]H. E. Stanley and J. Teixeira, J. Chem. Phys. **73** 3403 (1980).
[24]R. L. Blumberg, H. E. Stanley, A. Geiger, and P. Mausback, J. Chem. Phys. **80**, 5230 (1984).
[25]H. E. Stanley and A. Geiger, Phys. Rev. Lett. **49** 1749 (1982).
[26]F. H. Stillinger, Science **209**, 451 (1980).
[27]S. A. Rice and M. G. Sceats, J. Phys. Chem. **85**, 1108 (1981).
[28]R. J. Speedy, J. Phys. Chem. **88**, 3364 (1984).
[29]S. C. Mossop, Proc. Phys. Soc. London Sec. B **68**, 193 (1955).
[30]D. E. Hare and C. M. Sorensen, J. Chem. Phys. **87**, 4840 (1987).
[31]G. E. Walrafen and L. A. Blatz, J. Chem. Phys. **59**, 2646 (1973).
[32]G. W. Chantry, in *The Raman Effect*, edited by A. Anderson (Marcel Dekker, New York, 1971), Vol. 1.
[33]H. W. Schrotter, in *Raman Spectroscopy, Theory and Practice*, edited by H.A. Szymanski (Plenum, New York, 1970), Vol. 2.
[34]E. Whalley, Can. J. Chem, **55**, 3429 (1977).
[35]M. G. Sceats (personal communication).
[36]P. C. Li and J. P. Devlin, J. Chem. Phys. **59**, 547 (1973).
[37]J. P. Devlin (personal communication).
[38]T. C. Sivakumar, S. A. Rice, and M. G. Sceats, J. Chem. Phys. **39**, 3468 (1978).
[39]D. Bertolini, M. Cassettari, M. Ferrario, P. Grigolini, and G. Salvetti, Adv. Chem. Phys. **62**, 277 (1985).
[40]J. R Scherer, M. K. Go, and S. Kint, J. Phys. Chem. **78** 1304 (1974).